

## Electron refraction in ballistic electron-emission microscopy studied by a superlattice energy filter

J. Smoliner,\* R. Heer, C. Eder, and G. Strasser

*Institut für Festkörperelektronik & Mikrostrukturzentrum der TU-Wien, Floragasse 7, A-1040 Wien, Austria*

(Received 19 May 1998; revised manuscript received 30 June 1998)

Buried  $\text{Al}_{0.4}\text{Ga}_{0.6}\text{As}/\text{GaAs}$  superlattices on Au-GaAs Schottky diodes have been used as an energy filter to study the energetic current distribution in ballistic electron-emission microscopy (BEEM) at room temperature and  $T=100$  K. Due to the large difference in electron masses in Au and GaAs we find that parallel momentum conservation leads to considerable electron refraction at the Au-GaAs interface. As a consequence, the energetic distribution of the ballistic electron current is inverted beyond the Au-GaAs interface and an almost linear behavior of the BEEM spectrum is observed in the energetic regime of the superlattice miniband. [S0163-1829(98)51136-8]

Ballistic electron-emission microscopy<sup>1,2</sup> (BEEM) is a useful tool to study the local properties of semiconductor interfaces and buried structures. BEEM is a three terminal extension of conventional scanning tunneling microscopy (STM), where ballistic electrons are injected from a STM tip into a semiconductor via a thin metal base layer evaporated onto the sample. The corresponding ballistic electron current as a function of sample bias is called BEEM spectrum and is measured via a backside collector contact. In the BEEM spectrum, the onset bias of the BEEM current is only determined by the Schottky barrier height at the metal semiconductor interface. The local resolution of these measurements can be as good as 10 Å.

Originally, BEEM was only applied to determine metal-semiconductor Schottky barrier, heights and band-structure properties.<sup>3,4</sup> On GaP, e.g., the Schottky barrier heights for a large number of metals were determined by Ludeke, Prietsch, and Samsavar<sup>5</sup> and Prietsch and Ludeke.<sup>6</sup> Later, BEEM experiments were extended to higher bias voltages to study hot-electron effects such as impact ionization on GaP (Ref. 7) and silicon.<sup>8</sup> In the following, even a BEEM current induced adatom generation was observed.<sup>9</sup> As such effects are beyond the validity of the original Bell-Kaiser model,<sup>1,2</sup> Monte Carlo calculations were used to analyze these data quantitatively.<sup>10</sup>

After the Monte Carlo techniques worked well in the high bias regime, they were also applied to model the BEEM spectra in a voltage range close to threshold. Close to threshold, the Bell-Kaiser model<sup>1,2</sup> is usually a good description of the experimental data, however, it is not appropriate for samples on which elastic scattering in the metallic base plays a mayor role. This is of importance especially on the Au-Si (111) system, since here the electron needs a large transverse crystal momentum to enter the semiconductor.<sup>11,12</sup> It was also shown by Monte Carlo calculations that multiple electron reflections inside the metal have a strong influence<sup>13,14</sup> and that elastic scattering processes are the reason why the spectra for Au on Si(111) and Si(100) look so similar.<sup>15</sup>

In addition to surface properties, subsurface sample properties were also investigated by BEEM. On a GaAs/ $\text{Al}_x\text{Ga}_{1-x}\text{As}$  double barrier structure, e.g., it was possible to investigate the resonant states.<sup>16</sup> On self-assembled

InAs quantum dots,<sup>17,18</sup> the BEEM current was found to be enhanced, and even fine structure in the BEEM spectrum was discovered and attributed to the quantized states inside the dot. Motivated by these results, Monte Carlo simulations of the BEEM spectra for such buried mesoscopic structures were carried out in the following experiments.<sup>19</sup>

In our group, ballistic transport through the miniband of a GaAs- $\text{Al}_x\text{Ga}_{1-x}\text{As}$  superlattice was studied recently.<sup>20</sup> A miniband in a short period superlattice covers a rather broad energy range compared to a double barrier resonant tunneling diode and, therefore, electron transport through its states is more pronounced and better resolved. In our previous work, we have shown that the miniband results in a BEEM current threshold clearly below the height of the  $\text{Al}_x\text{Ga}_{1-x}\text{As}$  barriers and the peak in the second derivative of the BEEM spectrum was in good agreement with the calculated miniband position in the GaAs- $\text{Al}_x\text{Ga}_{1-x}\text{As}$  superlattice. In the present work, we analyze the spectral features of the measured BEEM on Au-GaAs Schottky diodes with a buried GaAs- $\text{Al}_x\text{Ga}_{1-x}\text{As}$  superlattice and show that due to parallel momentum conservation and electron refraction, the energetic distribution of the BEEM current is inverted beyond the Au-GaAs interface.

To study the energetic distribution of ballistic electrons by means of a superlattice energy filter, a 10 period 25-Å/30-Å  $\text{Al}_{0.4}\text{Ga}_{0.6}\text{As}/\text{GaAs}$  superlattice (SL) was grown by molecular beam epitaxy (MBE) on top of 600-Å undoped GaAs and a highly doped  $n$ -type collector region. To reduce the influence of the interface, the SL was followed by 300-Å undoped GaAs before finally capping it with an Au base layer. In order to provide "flatband" conditions at the Au/GaAs interface, a  $p$ -type  $\delta$ -doping ( $N_A=1.4\times 10^{12}$  cm<sup>-2</sup>) was inserted between the superlattice and the highly doped collector region. For the formation of minibands in the superlattice, these flatband conditions are essential, since an already small electric field can lead to localization effects in the superlattice, thus breaking up the miniband into single states. This flatband approach was first used by Sajoto *et al.*<sup>16</sup> as well as O'Shea *et al.*,<sup>21</sup> who studied single and double  $\text{Al}_x\text{Ga}_{1-x}\text{As}$  barriers buried in the semiconductor. Note that a (311)A substrate orientation was chosen to allow  $p$ -type doping using Si.

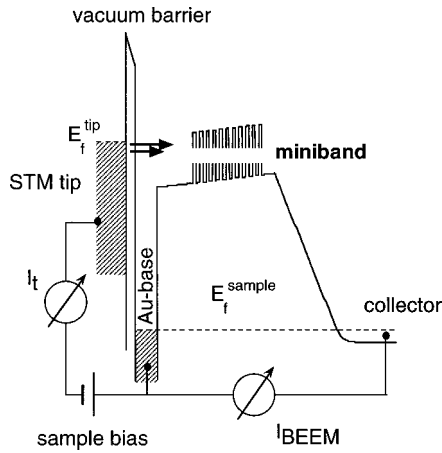


FIG. 1. Self-consistently calculated conduction-band profile of the Au-GaAs Schottky diodes with buried GaAs-Al<sub>x</sub>Ga<sub>1-x</sub>As superlattice.

Figure 1 shows a self-consistently calculated conduction-band profile<sup>22</sup> of our sample together with the experimental setup. Due to the special sample design, only one miniband exists in the superlattice. All other minibands are energetically above the Al<sub>x</sub>Ga<sub>1-x</sub>As barriers. The miniband covers an energy range from 1.02 to 1.09 eV at  $T=300$  K and a range from 1.06 to 1.14 eV at  $T=100$  K, respectively. As shown below, excellent agreement between the calculated and measured BEEM spectra is achieved for these values.

To prepare the samples for BEEM, a In/Sn backside contact was first alloyed in forming gas atmosphere. Then the samples were dipped into concentrated HCl solution for 30 s to remove the native thin oxide layer.<sup>23</sup> After rinsing the samples with deionized water they were immediately transferred into a evaporation unit. Finally an Au film (100 Å) was evaporated via a shadow mask. The size of the active area was  $0.2 \times 3$  mm<sup>2</sup>.

Figure 2 shows BEEM spectra measured at  $T=300$  and 100 K, which were obtained using a tunneling current of 5 nA in both cases. As one can see, the low-temperature BEEM spectrum is shifted to higher voltages. The corresponding threshold voltages are 0.91 V at  $T=300$  K and 1.01 V at  $T=100$  K, respectively. Two further features are evident in these spectra. First, the measured threshold voltage for BEEM current detection is clearly below the calculated

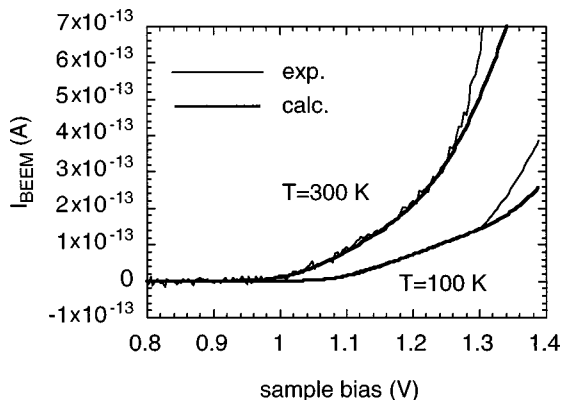


FIG. 2. Measured and calculated BEEM spectra at temperatures of  $T=300$  and 100 K, respectively. The transmission factors of the Au-base layer was  $t_0=1.5\%$  at  $T=300$  K and  $t_0=1.2\%$  at  $T=100$  K, respectively.

miniband position for the room-temperature spectrum. For the low-temperature spectrum, this effect is also observed, but less pronounced. The second unusual effect is most pronounced in the low-temperature spectrum. In contrast to Au-GaAs reference samples where the BEEM current follows a  $I_{\text{BEEM}} \propto (V - V_b)^{5/2}$  power law,<sup>24</sup> the spectrum of the superlattice sample is almost linear up to a sample bias of 1.3 V. Above that voltage, the electrons start to overcome the Al<sub>x</sub>Ga<sub>1-x</sub>As barriers of the superlattice and the BEEM current approximately follows the 5/2 power law observed on our reference samples.

The difference between the measured threshold voltages and the calculated miniband positions is qualitatively easy to understand. We first consider the situation at zero temperature: At  $T=0$  K, the electron distribution is sharply limited by the Fermi energy in the Au tip, and thus, the BEEM current will only be observed if the Fermi energy in the tip becomes higher than the miniband position. At elevated temperatures, this is no longer true, and already at  $T=100$  K, the broadening of the Fermi distribution function provides enough electrons for a BEEM current onset at voltages 40 meV ( $\approx 5$  kT) below the miniband position. At room temperature, this effect is even more pronounced, so that a BEEM current is already observed if the Fermi energy in the tip has overcome the Schottky barrier height at the Au-GaAs interface (0.92 eV).

The spectral behavior of the BEEM current and especially the linear increase above threshold, however, is intuitively unclear. To discuss this in more detail, we restrict ourselves to the voltage regime corresponding to energies above the Schottky barrier height at the Au-GaAs interface but below the top of the Al<sub>x</sub>Ga<sub>1-x</sub>As barriers of the superlattice. As the total energy of an electron, we define  $E = E_{\perp} + E_{\parallel}$ , where  $E_{\perp} = \hbar^2 k_{\perp}^2 / 2m^*$  and  $E_{\parallel} = \hbar^2 k_{\parallel}^2 / 2m^*$ .

For a given sample bias, electrons at the Fermi energy of the tip have the largest transmission coefficient through the vacuum barrier. Thus, most of the tunneling current and therefore most of the BEEM current is expected to flow at the Fermi energy. In the limit of zero temperature, this will lead to zero BEEM current for Fermi energies below the miniband position. As soon as the Fermi level crosses the miniband position, however, the BEEM current is expected to increase. For Fermi energies above the upper edge of the miniband, the BEEM current is expected to saturate, since the high-energy electrons are blocked by the Al<sub>x</sub>Ga<sub>1-x</sub>As barriers and the electrons at the energetic position of the superlattice miniband have always the same transmission coefficient. One mechanism, however, could in principle increase the BEEM current with increasing bias: At higher bias voltages and higher Fermi energies, the number of electrons in the energy range of the miniband increases due to higher possible values in  $E_{\parallel}$ . Due to parallel momentum conservation laws, however, the BEEM current does not increase, since the acceptance cone always limits the  $k_{\parallel}$  regime for electrons entering the semiconductor in the same way, no matter how large the Fermi energy is.

Experimentally, we do not observe a saturation in the BEEM current as a function of sample bias; we first assumed that inelastic scattering processes in the first 300 Å of GaAs in front of the superlattice are responsible for the observed linear increase of the BEEM current. Using the model of

Smith and Kogan,<sup>25</sup> however, we show below that the observed effect is quantitatively explained by electron refraction at the Au-GaAs interface and an inversion of energetic distribution of the BEEM current.

Smith and Kogan<sup>25</sup> developed their model to describe the BEEM spectra of buried heterostructures, such as the double barrier resonant tunneling diode used by Sajoto *et al.*<sup>16</sup> Essentially, their model is a modification of the original Bell-Kaiser model,<sup>2</sup> where the properties of the buried heterostructure are described by an additional transmission coefficient  $T(E_{\perp}, E_{\parallel})$  introduced into the numerator of the Bell-Kaiser formula. To analyze our superlattice data, we also used Smith and Kogan's approach. As in their work, we only considered transport in the  $\Gamma$  valley and have also included quantum-mechanical reflection. In addition, an experimentally measured voltage-dependent tip-sample separation was included too. The transmission coefficient of the superlattice was calculated numerically.

Figure 2 shows the measured BEEM spectra as well as the calculated spectra for temperatures of  $T=300$  and  $100$  K, respectively. The calculated curves show an excellent agreement with the experimental data for electron energies below the  $\text{Al}_x\text{Ga}_{1-x}\text{As}$  barrier height. The almost linear behavior for the low-temperature spectrum is also nicely reproduced. For electron energies above the  $\text{Al}_x\text{Ga}_{1-x}\text{As}$  barrier height, the calculated BEEM currents are too small. In our opinion, this clearly shows the influence of ballistic electron transport in higher valleys of GaAs, since a miniband existing in the  $L$  valley of the superlattice also coincides with the height of the  $\text{Al}_x\text{Ga}_{1-x}\text{As}$  barriers in the  $\Gamma$  valley.

After we have demonstrated that the model of Smith and Kogan describes well the data obtained on our superlattice sample, we now discuss the physical reasons for the almost linear behavior of the low-temperature BEEM spectrum. This linear behavior has two origins. First, the superlattice acting as  $k_{\perp}$  filter for ballistic electrons and, second, the parallel momentum conservation at the Au-GaAs interface at the sample surface. We now consider a single electron with given  $k_{\perp}^{\text{Au}}$  and  $k_{\parallel}^{\text{Au}}$  values in the Au film. If the electron crosses the interface, the large mass difference between the Au and the GaAs and parallel momentum conservation will lead to an electron refraction and, hence, to changes in  $k_{\perp}$  and  $E_{\perp}$ , respectively. As the mass in GaAs is much smaller than in Au an electron crossing the Au-GaAs interface will loose  $E_{\perp}$  and gain  $E_{\parallel}$  in GaAs according to

$$E_{\perp}^{\text{GaAs}} = E_{\perp}^{\text{Au}} - E_{\parallel}^{\text{Au}} \left( \frac{m_0}{m^*} - 1 \right), \quad (1)$$

where  $m_0$  is the free electron mass,  $m^*$  the effective mass in GaAs, and  $E_{\perp} = \hbar^2 k_{\perp}^2 / 2m^*$  is the component of electron energy perpendicular to the barriers. Although the total energy of the electron is conserved, this behavior has a dramatic influence on the transmission through the energy filter formed by the superlattice. To be transmitted through the superlattice, a proper value of  $E_{\perp}^{\text{GaAs}}$  is required, but depending on  $E_{\parallel}^{\text{GaAs}}$ , this electron will have a totally different energy  $E_{\perp}^{\text{Au}}$  in the Au film and will not be at the same energetic position as the miniband in the superlattice.

To demonstrate this influence of electron refraction in a quantitative way, we have calculated the quantity

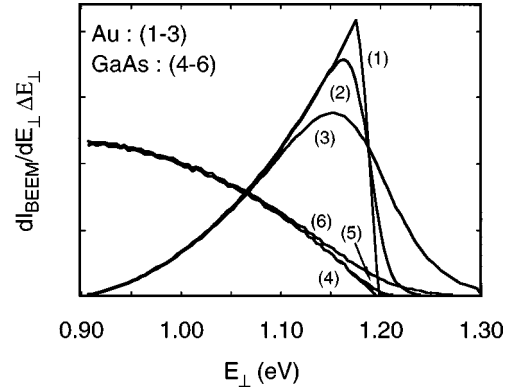


FIG. 3. BEEM current distribution per energy interval  $dI_{\text{BEEM}}/dE_{\perp} \Delta E_{\perp}$  as a function of electron energy. The sample bias was  $1.2$  V. Curves (1)–(3) represent the current distribution calculated on the Au side of the Au-GaAs interface for temperatures of  $T=4$ ,  $100$ , and  $300$  K, respectively. Curves (4)–(6) represent the corresponding current distribution in the GaAs.

$(dI_{\text{BEEM}}/dE_{\perp})\Delta E_{\perp}$ , which is a measure for that amount of BEEM current flowing in a given energy interval and thus reflects the energetic distribution of the ballistic electrons as a function of electron energy  $E_{\perp}$ . For this calculation we have chosen a sample bias of  $V=1.2$  V, which corresponds to a Fermi energy in the tip above the miniband position but below the  $\text{Al}_x\text{Ga}_{1-x}\text{As}$  barrier height. To show the influence of the refraction at the Au-GaAs interface, the current distribution was calculated on the Au- and GaAs side of the Au-GaAs interface. Figure 3 shows the result of this procedure. Curves (1)–(3) represent the energetic distribution of the BEEM current in the Au film calculated for temperatures of  $T=4$ ,  $100$  and  $300$  K, respectively. Due to the  $k_{\parallel}^{\text{Au}}$  restriction by the so-called acceptance cone,<sup>2</sup> the distribution is rather narrow and most of the BEEM current flows close to the Fermi energy. Curves (1)–(3) illustrate the broadening of the current distribution with increasing temperatures.

In the GaAs, the current distribution is practically inverted, which can be seen in curves (4)–(6) of Fig. 3. Due to  $k_{\parallel}$  conservation and “refraction” at the interface, a large number of electrons are transferred from high values of  $E_{\perp}$  in the Au film to lower values of  $E_{\perp}$  in GaAs, which explains why the expected saturation behavior of in the BEEM spectrum is not observed. If the sample bias is increased, an increasing number of electrons are transferred to lower  $E_{\perp}^{\text{GaAs}}$  values and, thus, the BEEM current in the energy window formed by the superlattice miniband increases continuously, leading to the almost linear increase of the BEEM current with increasing sample bias. Again, curves (4)–(6) illustrate the broadening of the current distribution due to elevated temperatures.

As shown above, our model gives an excellent description of our data, although scattering processes were completely ignored in our consideration. In the literature, however, elastic scattering processes such as multiple reflections inside the metal base<sup>11–15</sup> were found to be important. By elastic scattering processes, electrons can gain momentum  $k_{\perp}$  perpendicular to the superlattice, which in principle can explain the onset of BEEM current below the expected miniband position. By numerical simulations, however, we checked that scattering alone without refraction cannot explain the spectral behavior of our samples. Scattering alone just broadens

the energetic distribution of the BEEM current, similar to the way elevated temperatures affect the distribution in the Au film [see Fig. 3, curves (1)–(3)]. Thus, even strong elastic scattering will not lead to the “inversion” situation [Fig. 3, curves (4)–(6)] provided by the refraction effect. For the calculated spectrum this means that one will in fact obtain an earlier onset of the BEEM current but only a broad step instead of the experimentally observed linear behavior.

Although, in general, the  $k_{\parallel}$  conservation rule is assumed to be rigid, it is also sometimes a point of discussion in the literature. On the Au-Si system, e.g., there are hints that  $k_{\parallel}$  conservation must be relaxed,<sup>26</sup> but most recent publications show that this is not necessary to explain the results.<sup>15</sup> To check the influence of relaxed  $k_{\parallel}$  conservation rules for our samples, we have also carried out a simulation where the refraction effect was ignored and the  $k_{\parallel}$  conservation rules were relaxed by relaxing the energetic limitations of the acceptance cone. As a result we obtained that even in the case of a total relaxation of the  $k_{\parallel}$  conservation rule, a linear behavior is not achieved and a broad step is always obtained in the calculated BEEM spectrum.

From the above arguments we conclude that the refraction effect is the dominant mechanism in our sample and that scattering or relaxed  $k_{\parallel}$  conservation rules have only a minor influence. On the basis of the above model, however, one should be aware of some consequences for future BEEM experiments on “free-standing” subsurface structures such as superlattices or double barrier structures. Due to the tremendous broadening of the energetic BEEM current distribution through electron refraction at the Au-GaAs interface, resonant states in buried structures will only be visible as weak peaks in the second derivative of the BEEM spectrum. The use of base materials with small electron mass such as InAs,<sup>27</sup> can in principle help to circumvent this problem, since, in this case, the current distribution is focused by refraction at the InAs-GaAs interface. However, one should keep in mind that in this case a problem exists for the tun-

neling process between the tip and the InAs base. For tunneling processes, parallel momentum conservation laws are also valid, which, in planar tunneling theory, results in a rather broad energy distribution of electrons injected from a high mass tip into the small mass base material.

A different approach taken by Rubin *et al.*<sup>17</sup> circumvents this problem directly. They have investigated quantized states inside a self-assembled quantum dot, but in their sample, the quantum states were embedded in a surface depletion barrier and energetically located below the GaAs conduction band. Thus, ballistic electrons in the Au base can tunnel directly into or through the quantum dot states without being diffracted before, which obviously yields a much better energetic resolution. Of course, refraction will also occur as soon as the electrons leave the dot and enter the GaAs conduction band. In this case, however, electron refraction has no influence on the BEEM current, since the electrons are already in the collector electrode.

In summary, we have investigated ballistic electron transport through quantum states in buried GaAs-Al<sub>x</sub>Ga<sub>1-x</sub>As superlattices using ballistic electron-emission microscopy. Both at room temperature and  $T=100$  K, the miniband of the GaAs-Al<sub>x</sub>Ga<sub>1-x</sub>As superlattice adds spectral features to the measured BEEM current and quantitative agreement between the measured and calculated spectra was achieved using the model of Smith and Kogan. It was also shown that parallel momentum conservation at the Au-GaAs interface leads to electron refraction and inverts the energetic distribution of the ballistic electron current in the semiconductor. In our opinion, the resulting loss in energetic resolution for BEEM experiments can only be avoided, if a direct coupling between ballistic electrons in the metal base and the subsurface quantum states is achieved.

This work was sponsored by Oesterreichische Nationalbank, Project No. 6277, and Gesellschaft für Mikroelektronik (GME). The authors are grateful to E. Gornik for continuous support.

\*Electronic address: juergen.smoliner@tuwien.ac.at

<sup>1</sup>W. J. Kaiser and L. D. Bell, Phys. Rev. Lett. **60**, 1406 (1988).

<sup>2</sup>L. D. Bell and W. J. Kaiser, Phys. Rev. Lett. **61**, 2368 (1988).

<sup>3</sup>W. J. Kaiser, M. H. Hecht, L. D. Bell, F. J. Grunthaler, J. J. Liu, and L. C. Davis, Phys. Rev. B **48**, 18 324 (1993).

<sup>4</sup>H. Sirringhaus, E. Y. Lee, and H. von Känel, Phys. Rev. Lett. **73**, 577 (1994).

<sup>5</sup>R. Ludeke, M. Prietsch, and A. Samsavar, J. Vac. Sci. Technol. B **9**, 2342 (1991).

<sup>6</sup>M. Prietsch and R. Ludeke, Phys. Rev. Lett. **66**, 2511 (1991).

<sup>7</sup>R. Ludeke, Phys. Rev. Lett. **70**, 214 (1993).

<sup>8</sup>A. Bauer and R. Ludeke, Phys. Rev. Lett. **72**, 928 (1994).

<sup>9</sup>H. D. Hallen, T. Huang, A. Fernandez, J. Silcox, and R. A. Burman, Phys. Rev. Lett. **69**, 2931 (1992).

<sup>10</sup>A. Bauer, M. T. Cuberes, M. Prietsch, and G. Kaindl, Phys. Rev. Lett. **71**, 149 (1993).

<sup>11</sup>L. J. Schowalter and Y. Lee, Phys. Rev. B **43**, 9308 (1991).

<sup>12</sup>F. J. Garcia-Vidal, P. L. de Andres, and F. Flores, Phys. Rev. Lett. **76**, 807 (1996).

<sup>13</sup>L. D. Bell, Phys. Rev. Lett. **77**, 3893 (1996).

<sup>14</sup>C. Manke, Y. Bodschwinn, and M. Schulz, Appl. Surf. Sci. **117/118**, 321 (1997).

<sup>15</sup>P. L. de Andres, K. Reuter, F. J. Garcia-Vidal, D. Sestovic, and F. Flores, Appl. Surf. Sci. **123/124**, 199 (1998).

<sup>16</sup>T. Sajoto, J. J. O'Shea, S. Bhargava, D. Leonard, M. A. Chin, and V. Narayanamurti, Phys. Rev. B **74**, 3427 (1995).

<sup>17</sup>M. E. Rubin, G. Medeiros-Ribeiro, J. J. O'Shea, M. A. Chin, E. Y. Lee, P. M. Petroff, and V. Narayanamurti, Phys. Rev. Lett. **77**, 5268 (1996).

<sup>18</sup>W. Wu, J. R. Tucker, G. S. Solomon, and J. S. Harris, Jr., Appl. Phys. Lett. **71**, 1083 (1997).

<sup>19</sup>E. Y. Lee, V. Narayanamurti, and D. L. Smith, Phys. Rev. B **55**, R16 033 (1997).

<sup>20</sup>C. Eder, J. Smoliner, R. Heer, G. Strasser, and E. Gornik, Physica E **12**, 850 (1998).

<sup>21</sup>J. J. O'Shea, T. Sayoto, S. Bhargava, D. Leonard, M. A. Chin, and V. Narayanamurti, J. Vac. Sci. Technol. B **12**, 2625 (1994).

<sup>22</sup>G. Snider (unpublished).

<sup>23</sup>A. A. Talin, D. A. Ohlberg, R. S. Williams, P. Sullivan, I. Koutselas, B. Williams, and K. L. Kavanagh, Appl. Phys. Lett. **62**, 2965 (1993).

<sup>24</sup>C. Eder, J. Smoliner, G. Strasser, and E. Gornik, Appl. Phys. Lett. **69**, 1725 (1996).

<sup>25</sup>D. L. Smith and Sh. M. Kogan, Phys. Rev. B **54**, 10 354 (1996).

<sup>26</sup>R. Ludeke and R. Bauer, Phys. Rev. Lett. **71**, 1760 (1993).

<sup>27</sup>R. Heer, J. Smoliner, G. Strasser, and E. Gornik, Appl. Phys. Lett. **73**, 1218 (1998).